Journal of Materials Chemistry A

Accepted Manuscript

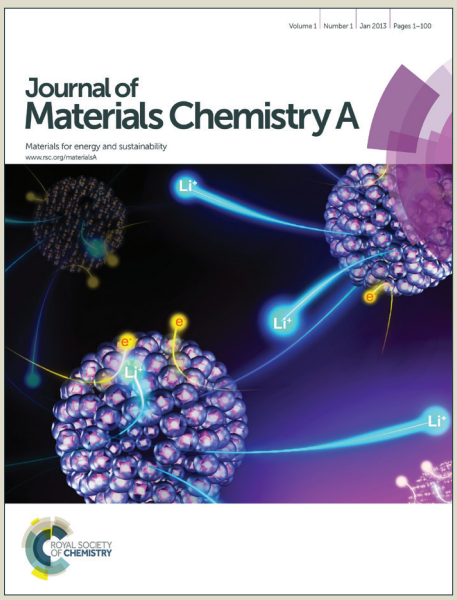

ROYAL SOCIETY OF CHEMISTRY

www.rsc.org/materialsA

Journal of Material Chemistry A

ARTICLE

At the Polymer Electrolyte Interfaces: the Role of the Polymer Host for Interphase Layer Formation in Li-Batteries

Received 00th January 20xx,
Accepted 00th January 20xx

DOI: 10.1039/x0xx00000x

www.rsc.org/

Bing Sun, Chao Xu, Jonas Mindemark, Torbjörn Gustafsson, Kristina Edström, Daniel Brandell*

In this study, X-ray photoelectron spectroscopy was applied for compositional analysis of the interphase layers formed in graphite and $LiFePO_4$ Li-battery half cells containing solid polymer electrolytes (SPEs) consisting of poly(trimethylene carbonate) (PTMC) and LiTFSI salt. Decomposition of PTMC was observed at the anode/SPE interface, indicating different reaction products than those associated with the more conventional host material poly(ethylene oxide). Degradation mechanisms of the PTMC host material at low potentials are proposed. Compared to the $LiFePO_4$/PEO interface, an absence of LiOH – a result of water contaminations – was generally seen when using hydrophobic PTMC as the polymer host. A clear correlation of moisture content with the constitution of interphase layers in Li polymer batteries could thus be concluded. At the SPE/$LiFePO_4$ interface, good stability was seen regardless of the polymer host materials.

Introduction

The safety in energy storage devices for conventional consumer electronics (e.g., cell phones and laptops) or large-scale energy storage units for electric grids and vehicles has become a prioritized concern for the choice of power sources.[1–4] Battery chemistries which are not only chemically inert and electrochemically stable, but also display long-term performance, are pressingly demanded. Recent years have seen significant success in the development of different Li-ion battery electrodes for high energy and/or high power applications, and major advances in the area can be foreseen.[5–8] On the other hand, challenges remain in the development of electrolytes, especially to tackle the compatibility with the more extreme electrode potentials currently being employed and the corresponding stability at the electrode/electrolyte interfaces.[9–13]

Safe batteries would favorably comprise non-flammable and chemically stable electrolyte materials with wide electrochemical windows to suppress electrolyte decomposition and unwanted side-reactions.[9,10,12] Within this context, solid-state electrolyte systems, such as solid (solvent-free) polymer electrolytes (SPEs), stand out due to their intrinsic chemical inertness, good electrochemical, thermal and mechanical stability as compared to conventional liquid electrolytes.[14–17] Their better mechanical flexibility also render them more easily employed with conventional Li-battery electrodes, as compared to ceramic systems. With obvious advantages for simple and flexible battery designs, polyether-based SPEs (e.g., polyethylene oxide; PEO) have demonstrated potential usefulness through a diverse material design via synthetic modifications to achieve improved electrochemical and chemical properties for both Li- and Li-ion batteries.[18–24]

There are, however, a number of intrinsic problems with polyethers – such as limited amorphicity and a poor Li transference number – which may be overcome by employment of alternative polymer hosts.[25–27] A promising alternative in this context is polycarbonates, which have been studied as Li-ion conductors in recent years by a limited number of groups and demonstrated good electrochemical stability (up to 5 V vs. Li^+/Li) and favorable Li-salt solvation.[28–34] Our recent studies on electrolytes of the rather hydrophobic poly(trimethylene carbonate) (PTMC) materials and its oligomer displayed long-term cyclability and reasonable rate capability in $LiFePO_4$-cells.[29,30] A high practical capacity of close to 153 mAh g^{-1} was achieved for above 100 cycles. Further development via copolymerization of TMC and ε-caprolactone (CL) yielded large improvements of ionic conductivity in the SPEs (in the range of 10^{-4}–10^{-5} Scm^{-1} at 60 °C), which rendered good capacity retention and rate capability (150–140 mAh g^{-1} at 60 °C for C/20 and C/5, respectively).[31]

For battery performance under practical operation conditions, the role of the Solid Electrolyte Interphase (SEI) on the anode side and Solid Permeable Interphase (SPI) on the cathode side have been recognized decisive in terms of capacity retention, safety and battery life span.[12,35–40] The work in this field has dominantly been devoted to liquid (or gel) electrolytes containing linear and cyclic carbonate solvents, mostly at the anode side (e.g., on Li metal or graphite), while X-ray photoelectron spectroscopy (XPS) has evolved to become the standard methodology in these investigations.[41–44] Structurally, the SEI formed in liquid electrolytes is considered to be an electronically insulating layer consisting of organic/inorganic multilayers; an inner layer containing inorganic composites (e.g., LiF, Li_2O, Li_2CO_3) and an outer layer mainly comprising oligomers or polymers.[45–47] Both computational and experimental studies also suggested the ionic conductivity of these layers to be in the order of 10^{-8} to 10^{-10} S cm^{-1} at RT,[48] which is similar to the properties expected in typical solid (polymer) electrolytes.

Department of Chemistry – Ångström Laboratory, Uppsala University, Box 538, SE 75121, Uppsala, Sweden. Email: daniel.brandell@kemi.uu.se

† Electronic Supplementary Information (ESI) available. See DOI: 10.1039/x0xx00000x

As compared to their liquid counterparts, the interfacial chemistry in Li- and Li-ion polymer batteries using SPEs has been much less explored. This is perhaps partly due to the common belief that solid polymers are generally more chemically and electrochemically stable than liquid solvents, but also due to technical difficulties to directly probe the composition of electrode/SPE interfaces originating in the comparably strong attachment of the SPE material to the electrode surface. Previous studies using in-situ electrochemical impedance analysis (EIS) has shown the evolution of interfacial resistance at the Li/SPE interface.[49–51] This indicated the formation and evolution of interphase layers in Li polymer batteries during electrochemical cycling and/or varied state-of-charge. However, a direct estimation of the composition for these layers formed at electrode surfaces can only be achieved using XPS. Our previous report on the XPS study of Li|PEO-LiTFSI|graphite half cells constituted one such first attempt, and revealed obvious compositional difference at the interfaces as compared to battery cells cycled with liquid electrolyte (i.e., EC:DEC=2:1, 1 M LiTFSI).[52] It was also shown that the high moisture content in PEO-LiTFSI was critical for in the SEI layer formation. Both PEO and LiTFSI are known to be hygroscopic, and it has also been pointed out from spectroscopy studies that water absorbed in a poly(ethylene glycol) (PEG) matrix could not be removed simply through conventional thermal treatment.[53] The large amount of LiOH detected on the graphite surface can therefore be considered closely correlated to the high moisture content in the SPEs.[52]

Our previous XPS study has only explored one electrolyte material, and only for anode interfaces. Moreover, the stability of SPEs on cathode interfaces has also been questioned in literature.[12,13] This present work thus investigates a less hygroscopic SPE system based on polycarbonates, and also for the cathode side interfaces. Compared to the 'hydrated' PEO-LiTFSI system, with water contents of hundreds up to thousands of ppm, much less moisture uptake (<40 ppm) was detected in the PTMC-LiTFSI system by Karl-Fischer titration. This will provide information on how the interphase layers are formed using 'dry' SPE materials. Moreover, considering the structural similarity between polycarbonates and their liquid analogues, e.g., linear and cyclic carbonates, examinations of the electrochemical performance and the possible degradation routes of PTMC-based SPEs are of great interest. XPS has therefore been applied to depict the SEI and SPI compositions at the electrode/SPE interfaces.

Experimental

Solid polymer electrolyte preparation

Self-standing SPE samples of both PTMC and PEO doped with LiTFSI were prepared using solution-casting and a routine drying procedure described elsewhere.[31] Salt concentrations generating optimal conductivities were employed: [TMC]:[Li^+] = 8:1 for $PTMC_8$LITFSI and [EO]:[Li^+] = 25:1 for PEO_{25}LiTFSI, respectively. All sample preparations were performed in a glove box (H_2O<1 ppm, O_2<1 ppm).

XPS sample preparation and characterization

The preparation of composite electrodes has been described elsewhere.[30,52] All electrodes (diameter of 12 mm) were dried at 120 °C for 12 h in a vacuum oven. A pouch cell configuration was used for cell assembly in which the self-standing SPE was sandwiched between a composite electrode and a Li foil (CYPRUS Foote Mineral Co.). All samples were pre-stored in an oven at 50 °C for 6 h prior to cycling. The $LiFePO_4$ half cells using either PEO_{25}LiTFSI or $PTMC_8$LiTFSI were cycled on a VMP2 (Biologic) till the 1st discharged state (i.e., at 0.01 V vs. Li^+/Li when fully delithiated) between 2.7 and 3.7 V vs. Li^+/Li at C-rate of C/50 at 50 °C. For comparison, a $LiFePO_4$ half cell employing acetate-terminated PTMC oligomer at the $LiFePO_4$/PTMC-LiTFSI interface was examined after 50 cycles (cell assembly details and cell performance described elsewhere).[29] The use of the oligomer was found to greatly facilitate the cell disassembly to expose the interfaces after long cycling and still provided comparable characteristics with the bulk SPE. The graphite half cell was cycled from its open circuit voltage till its 1st discharge state at 0.01 V vs. Li^+/Li (i.e., fully lithiated state) at a C-rate of C/50 at 50 °C. There were four interfaces examined per half cell, i.e., the composite electrode surface and the SPE surface in contact with it, as well as the Li metal surface and the SPE surface attached to it.

XPS characterization was carried out on a PHI 5500 system using monochromatized AlKα (hv=1487 eV) as the incident source. This allows a probing depth of around 10 nm. Samples were carefully transferred with a delicate transfer chamber to avoid moisture and air contamination. An electron neutralizer was employed to compensate charging on SPE surfaces. The obtained spectra were all curve-fitted with CasaXPS using 70 % Gaussian and 30 % Lorentzian Voigt peak shapes. Calibration was applied using the hydrocarbon peak at 285 eV and all spectra were normalized by the area of the respective core level signal. 1.2 eV was used as the S2p spin-spin splitting energy.

Results and Discussion

Graphite/PTMC-LiTFSI/Li interfaces

Fig. 1 displays XPS signals from the graphite/PTMC–LiTFSI interface after the 1st cycle, revealing information on the SEI layer formed. As compared to our observations on the graphite/PEO interface,[52] components such as Li_2O (at 528.4 eV in the O1s spectrum) appear to be formed solely in the PTMC system, while this compound would decompose to form LiOH for the water-contaminated PEO-based SPEs. Considering the small amount of H_2O detected in the 'dry' PTMC polymer, LiOH (reference values of 530–531 eV[43,52]) is not expected to be the dominating SEI component in the polycarbonate. The peaks positioned around 531 eV (at 531.6 eV and 530.7 eV, respectively) in the O1s spectrum are therefore instead proposed to be PTMC-derived Li alkyl carbonate and Li alkoxide (denoted PTMC-Li-C and PTMC-Li-A, respectively). The possible compounds formed from polymer decomposition are also significantly different for the PTMC and PEO polymer hosts, although these C1s and O1s signals corresponding to polymer degradation products were difficult to resolve for PEO-based electrolytes. Salt decomposition products, e.g., LiF, Li_3N and sulfur-species (Li_2S, Li_2SO_3, polysulfur and polysulfide), were also detected in the corresponding F1s, N1s and S2p spectra at both surfaces. These components are consistent with the signals seen at graphite/PEO interfaces,[52] indicating TFSI anion decomposition. Moreover, the Li_xC signal observed in the C1s spectrum is typical for lithiated graphite.[43,52] A comparison of the species on the two different PTMC and graphite surfaces shows that the signal from Li_2O could be barely seen at the graphite surface, accompanied with a slightly less pronounced Li_3N signal, while more strongly pronounced signals from sulfur species at close to 160 eV (i.e., Li_2S) were observed. This might be due to specific characteristics of the graphite electrode (e.g., surface functionality),[36,41,46] which

catalyses severe salt degradation on the graphite surface in contact with either PEO–LiTFSI[52] or the PTMC–LiTFSI electrolyte investigated here. A complete list of binding energy assignments of the anode SEI components as well as pristine compounds is described in **Table 1**, and an overall summary of the atomic concentration of the respective element from all the samples is listed in the ESI (**Table S1**).

The degradation mechanism of liquid carbonate solvents (e.g., propylene carbonate; PC) at low potentials in Li- and Li-ion batteries has been well discussed.[45,54,55] Considering the structural similarity of these solvents to the polymer host investigated here, it is highly plausible that similar reactions may also be relevant to describe the degradation of the PTMC backbone. As shown in **Scheme 1,** possible degradation can be initiated by a one-electron reduction of PTMC. This could conceivably occur in two ways to form either the PTMC Li carbonate (PTMC-Li-C), by splicing off a radical PTMC fragment, or a carboxyl radical by splicing off a Li alkoxide (PTMC-Li-A). The PTMC Li carbonate can then be decarboxylated either chemically (forming CO_2) or electrochemically (forming a Li carbon dioxide radical) to produce the PTMC-Li-A. This can also be formed from the intermediate from the second reduction pathway by another one-electron reduction, splicing off carbon monoxide. This is analogous to the established chemical and electrochemical degradation pathways of dimethyl carbonate.[56] Further polymer degradation can occur chemically through transesterification by

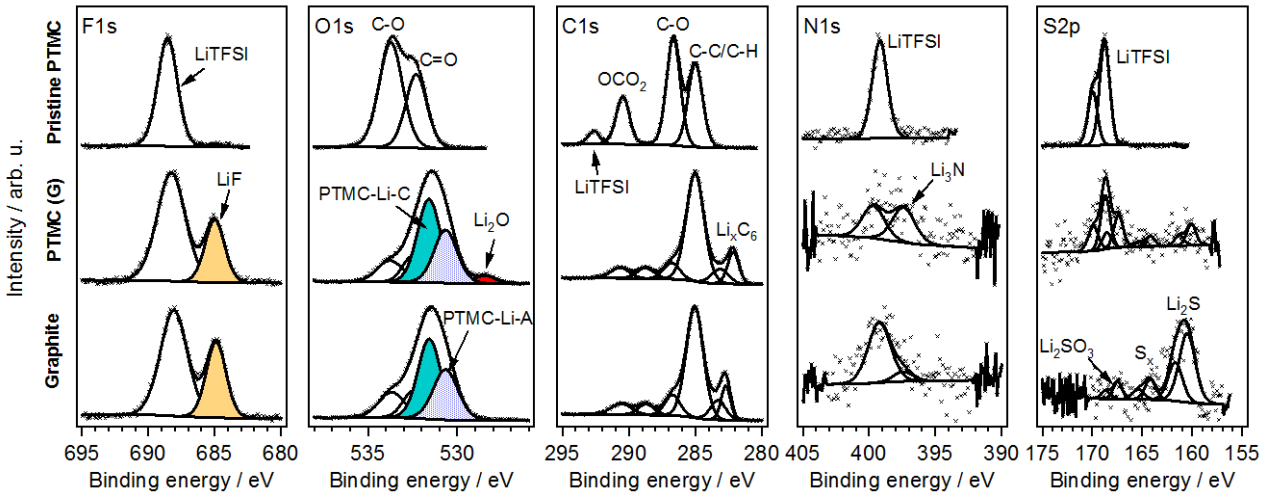

Fig. 1 XPS spectra showing the elemental fittings from the graphite/SPE surfaces of a graphite/PTMC$_8$LiTFSI/Li half cell cycled to the 1st discharge at 0.01 V vs. Li$^+$/Li using a C-rate of C/50 at 50 °C.

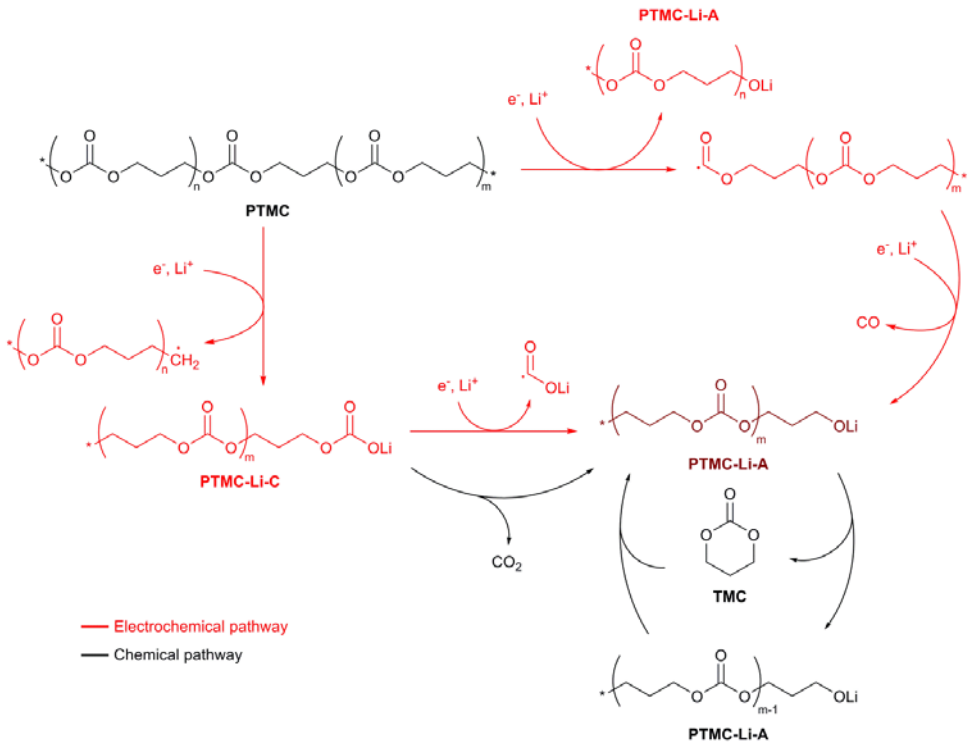

Scheme 1 Schematic illustration of possible chemical and electrochemical degradation pathways of high-molecular-weight PTMC during electrochemical cycling. The end-groups of the PTMC backbone have been omitted for clarity, unless explicitly written out.

means of a nucleophilic attack of end-group alkoxide of PMTC-Li-A on the carbonyl carbon of nearby carbonate groups. If this occurs intermolecularly, the molecular weights of the polymers will be scrambled but no new unique species will be formed. Intramolecular transesterification, on the other hand, may splice off one repeating unit in the form of the cyclic monomer trimethylene carbonate (TMC), which will exist in equilibrium with PTMC-Li-A as shown in **Scheme 1**. The TMC monomer could also react electrochemically and be reduced in a manner analogous to the degradation of ethylene carbonate (EC).[45,54] It is unlikely that any major concentration of the monomer would ever accumulate and it might not be possible to detect any of its degradation products. The scheme presented should be valid in a properly water-free system, otherwise there could also be secondary reactions between PTMC-Li-C and water to form Li_2CO_3.[57] It is worth to note that Li_2CO_3 (reference values of 290 eV in the C1s spectrum and 532 eV in the O1s spectrum[52,58]) was not detected at any of the surfaces. The hydroxyl end-groups of PTMC might also to some extent contribute to the decomposition. They should, however, barely play a noticeable role in such a high-molecular-weight polymer where the end-group concentration (and the concentration of their degradation products) is negligible. On a similar note, while the solid degradation products deposited on the examined surfaces can be detected spectroscopically, detection of the gaseous CO and CO_2 formed in the proposed reaction scheme would be much more difficult. This is particularly true for an SPE system, where the electrolyte/electrode interface is solid and stationary, leading to degradation taking place only in a very thin interfacial layer and producing only small amounts of the degradation products. Gaseous species, such as the aforementioned CO and CO_2, will not deposit on the surface, but rather dissolve into the SPE, thus preventing detection at the interface by spectroscopic methods.

Degradation of the PEO host material has previously been confirmed in graphite half cells,[52] and it is difficult to assess using the more qualitative XPS technique which of the polymer host that degrades to a higher extent. Furthermore, overlapping signals were seen for PEO together with those from hydrocarbons (at 285 eV in the C1s spectrum) and were thus difficult to differentiate. Also, salt degradation products were confirmed for both the PTMC–LiTFSI and the PEO–LiTFSI systems at the interface with the graphite electrode, and both SPEs were showing pronounced decomposition especially on the graphite surface as compared to the SPE surface. This suggests that LiTFSI degradation is a common phenomenon in graphite/SPE-based half cells following the same degradation mechanisms as proposed in our previous work.[52]

$LiFePO_4$/SPE/Li interfaces

Fig. 2 and **Fig. 3** display XPS data from interphase layers formed in $LiFePO_4$ half cells containing either PTMC- or PEO-based SPEs, for $LiFePO_4$/PTMC and PTMC/Li interfaces after the first discharge. At the Li/PTMC–LiTFSI interface, there are small amounts of LiF and Li_2S detected, originating from decomposed salt. At the cycled Li metal surface, signals of carbonate species, likely Li_2CO_3 as indicated by the C1s peak at 290.0 eV and the O1s peak at 531.6 eV, could be originating from the pristine Li metal.[52] The weak signal of Li_2O at 528.4 eV in the O1s spectrum is a feature originating from pristine Li metal.[35] Decomposed PTMC species, Li alkyl carbonate and Li alkoxide, were found close to the Li metal surface, indicating that the proposed polymer degradation reactions for graphite SEI formation may also be valid here, and might well occur generally for PTMC at low electrochemical potentials. It should be mentioned that salt signals were seen from all surfaces. Adhesion of the polymer electrolyte to the composite electrode after cycling was commonly observed during the disassembly of SPE-based cells.[52] Unlike the common treatment of electrodes in liquid electrolyte-based cells, no washing procedure was applied before the measurements.

In contrast, LiF was barely observed at the PTMC/$LiFePO_4$ interfaces. A long-cycled $LiFePO_4$ half cell employing acetate-terminated PTMC oligomers at the $LiFePO_4$/PTMC-LiTFSI interface was also examined after 50 cycles (cell assembly and performance described elsewhere).[29] The use of the oligomer was found to greatly facilitate the cell disassembly to expose the interfaces after

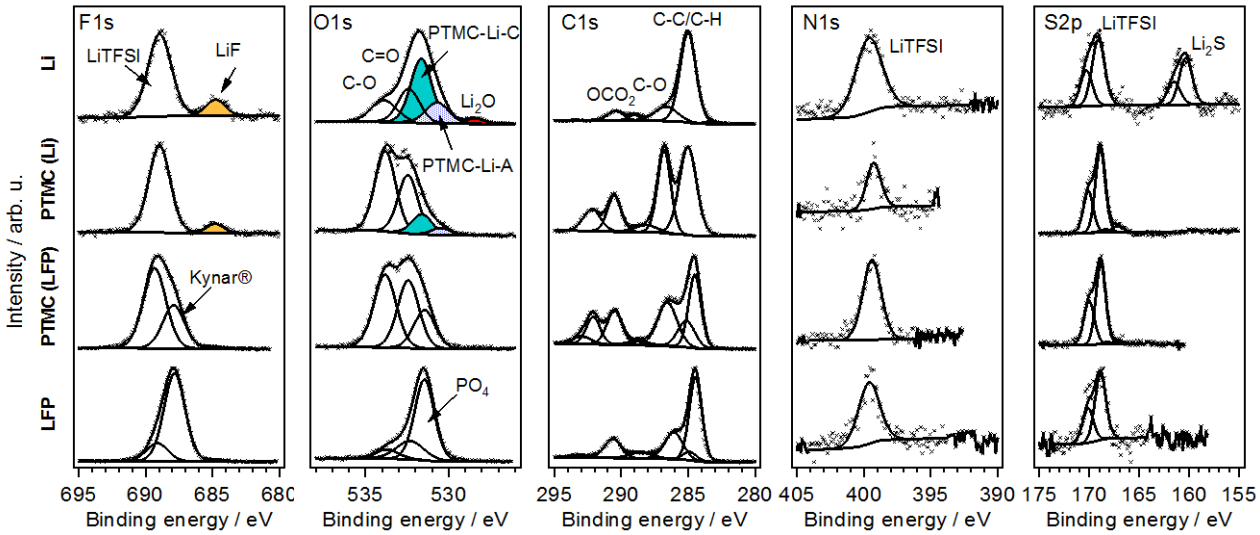

Fig. 2 XPS spectra showing the elemental fittings from the examined surfaces from a $LiFePO_4$/$PTMC_8$LiTFSI/Li half cell after the 1st discharge cycle.

Table 1 Binding energy assignments of curve fitted peaks from graphite and $LiFePO_4$ half cells containing $PTMC_8LiTFSI$.

Components		Binding Energy (eV)				
		C1s	O1s	F1s	N1s	S2p$_{3/2}$
Pristine materials	Hydrocarbon	285.0				
	C=O (PTMC)	290.4	532.3			
	C–O (PTMC)	286.6	533.7			
	Kynar 2801®	286.3; 288.6 290.8; 293.4		689.5; 687.6		
	LiTFSI	292.6		688.5	399.3	168.7
	Graphite	284.5				
Interphasial species	Li_2O		528.4			
	ROLi (PTMC-Li-A)		530.7			
	$ROCO_2Li$(PTMC-Li-C)		531.6			
	Li_xC	282.9; 283.1				
	Li_3N				396.9	
	LiF			684.9		
	Li_2SO_3					167.5
	Li_2S					160.5
	Polysulfur or polysulfide					163.7

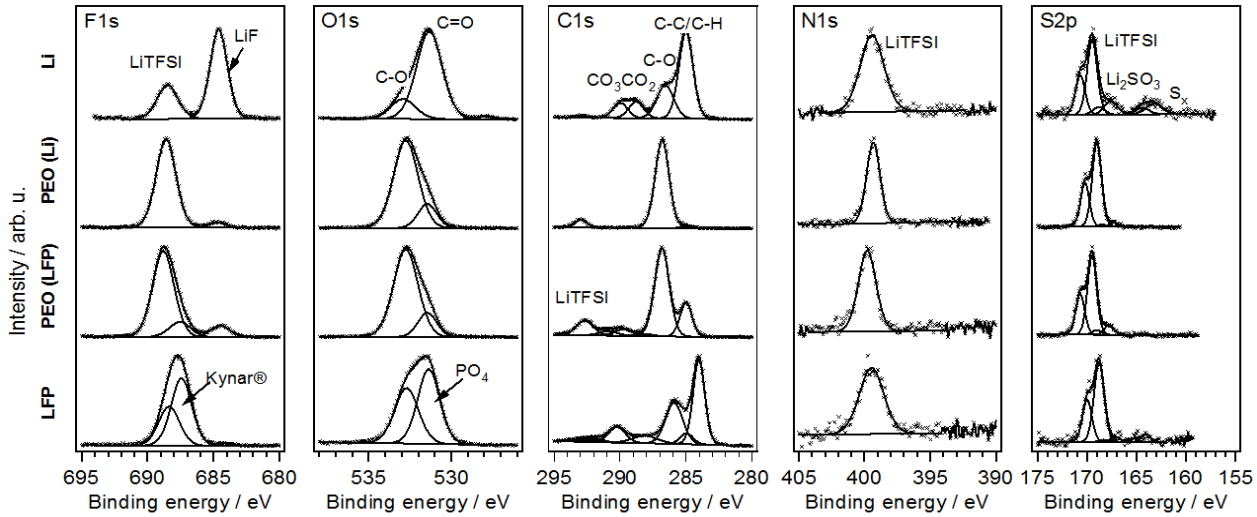

Fig. 3 XPS spectra showing elemental fittings from the respective surfaces of a $LiFePO_4/PEO_{25}LiTFSI/Li$ half cell after the first discharge.

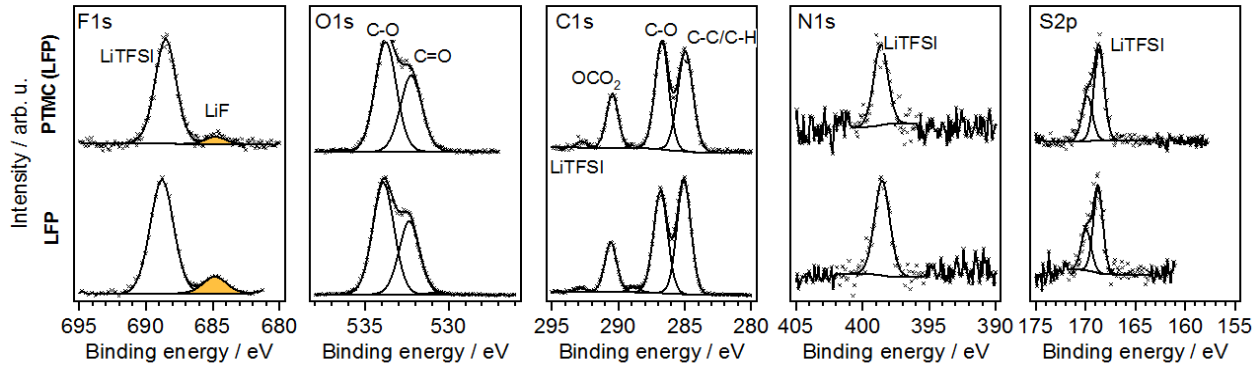

Fig. 4 XPS spectra showing elemental fittings from the respective surfaces of a $LiFePO_4/PTMC_8LiTFSI$+oPTMC/Li half cell after 50 cycles.

long cycling and still provided comparable characteristics with the

bulk SPE. XPS spectra from this sample are shown in **Figs. 4** and those from the pristine electrodes are provided in the ESI (**Fig. S1**).

In this long-cycled cell, trace amounts of LiF were observed at the PTMC/$LiFePO_4$ interface. Since the solubility of LiF is notably low in organic solvents and in common polymer host materials,[14,59] it is unlikely that the LiF traces found on the cathode side would have originated at the PTMC/Li interface and diffused through the SPE membrane. Rather, it appears that LiF is continually formed at the SPE/$LiFePO_4$ interface from salt and/or binder decomposition at a rate that is too low for it to be detectable after a single cycle. With extended cycling, this accumulates to the point where it can be seen in the spectra. The limited degradation observed further confirms the good chemical/electrochemical stability of the $LiFePO_4$/PTMC interface.

For comparison, a PEO-based $LiFePO_4$ half cell was also examined (**Fig. 3**). Apart from a slight variation in the amount of the salt residuals, which might well be due to inhomogeneous salt decomposition across the interfaces,[60] a general agreement regarding the SPI composition could be seen at the cathode side when comparing the PTMC– and PEO–LiTFSI systems.

Conclusions

In conclusion, hydrophobic PTMC host materials doped with LiTFSI have here been employed as SPEs and compared to conventional PEO-based electrolytes. At the graphite/PTMC-LiTFSI interface, the SEI layer close to the graphite surface was found to mainly consist of decomposed products (e.g., LiF, Li_2S, Li_2SO_3, Li_3N) which are likely formed from the salt and/or the binder, which are comparable to those observed in the 'hydrated' PEO system. Both polymer hosts also display polymer degradation products on the anode side; PTMC-derived Li alkyl carbonate and Li alkoxide are proposed to be the key products formed at the graphite interface for PTMC–LiTFSI. These are suggested to be formed through a series of electrochemical/chemical degradation processes following a similar degradation scheme as observed for linear carbonate solvents. However, the large proportions of LiOH from water contaminants found in PEO-based systems are more or less absent for PTMC. It is not clear at this moment what implications this has for the properties and stability of the SEI layer, but it is reasonable to assume that the absence of such a pronounced feature would notably affect the characteristics of the SEI. In this respect, further studies are necessary to explore how this difference in SEI layer formation influences the long-term cycling of SPE-based batteries. The extra components of LiOH for PEO-based SPEs will likely contribute to an increased interfacial resistance, but might also provide a protective layer on the active anode material. The $LiFePO_4$/SPE interface, on the other hand, appeared to be stable regardless of polymer host, with only small amounts of LiF and salt decomposition products detected, showing that the stability of SPEs at the cathode side is perhaps of no immediate concern when constructing safer Li-batteries. The salt decomposition might be a concern for the SEI formation at the anode/SPE interface, though it is still not clearly understood if the TFSI anion plays any role in polymer degradation. Future developments via a suitable selection of salt – or additives to stabilize the anode/SPE interfaces – may be critical for realization of all-solid-state Li-batteries.

Acknowledgements

The acknowledgements come at the end of an article after the This research has been financed by STandUP for Energy, the Swedish Energy Agency (grant agreement 34191-1) and the Swedish Research Council (grant no. 2012-3837).

Notes and references

1. M. Armand and J.-M. Tarascon, *Nature*, 2008, **451**, 652–657.
2. D. Aurbach, Y. Talyosef, B. Markovsky, E. Markevich, E. Zinigrad, L. Asraf, J. S. Gnanaraj, and H.-J. Kim, *Electrochim. Acta*, 2004, **50**, 247–254.
3. P. G. Balakrishnan, R. Ramesh, and T. Prem Kumar, *J. Power Sources*, 2006, **155**, 401–414.
4. E. P. Roth and C. J. Orendorff, *Electrochem. Soc. Interface*, 2012, 45–49.
5. A. S. Aricò, P. Bruce, B. Scrosati, J. Tarascon, and W. Van Schalkwijk, *Nat. Mater.*, 2005, **4**, 366–377.
6. S. Tan, Y. J. Ji, Z. R. Zhang, and Y. Yang, *Chem. Phys. Chem.*, 2014, **15**, 1956–1969.
7. S. K. Cheah, E. Perre, M. Rooth, M. Fondell, A. Hårsta, L. Nyholm, M. Boman, J. Lu, P. Simon, and K. Edström, *Nano Lett.*, 2009, **9**, 3230–3233.
8. H. Li, Z. Wang, L. Chen, and X. Huang, *Adv. Mater.*, 2009, **21**, 4593–4607.
9. E. Quartarone and P. Mustarelli, *Chem. Soc. Rev.*, 2011, **40**, 2525–2540.
10. E. S. Steven, J. B. Kerr, and K. Kim, *J. Power Sources*, 2003, **119-121**, 330–337.
11. J.-M. Tarascon, *Phil. Trans. R. Soc. A*, 2010, **368**, 3227–41.
12. K. Xu, *Chem. Rev.*, 2014, **114**, 11503–11618.
13. K. Xu, *Chem. Rev.*, 2004, **104**, 4303–417.
14. M. B. Armand, *Annu. Rev. Mater. Res.*, 1986, **16**, 245–261.
15. D. T. Hallinan and N. P. Balsara, *Annu. Rev. Mater. Res.*, 2013, **43**, 503–525.
16. W. H. Meyer, *Adv. Mater.*, 1998, **10**, 439–448.
17. A. Manuel Stephan and K. S. Nahm, *Polymer*, 2006, **47**, 5952–5964.
18. F. Croce, G. B. Appetecchi, L. Persi, and B. Scrosati, *Nature*, 1998, **394**, 456–458.
19. A. Ghosh, C. Wang, and P. Kofinas, *J. Electrochem. Soc.*, 2010, **157**, A846–A849.
20. P. P. Soo, *J. Electrochem. Soc.*, 1999, **146**, 32–37.
21. C. Wang, T. Sakai, O. Watanabe, K. Hirahara, and T. Nakanishi, *J. Electrochem. Soc.*, 2003, **150**, A1166.
22. H. Xiong, H. Xiong, H. Zhang, H. Zhang, J. Chen, and J. Chen, *J. Mater. Chem.*, 2004, **14**, 2775–2780.
23. H. Xiong, X. Zhao, and J. Chen, *J. Phys. Chem. B*, 2001, **105**, 10169–10174.
24. B. Sun, I.-Y. Liao, S. Tan, T. Bowden, and D. Brandell, *J. Power Sources*, 2013, **238**, 435–441.
25. O. Buriez, Y. B. Han, J. Hou, J. B. Kerr, J. Qiao, S. E. Sloop, M. Tian, and S. Wang, *J. Power Sources*, 2000, **89**, 149–155.
26. M. A. Ratner, P. Johansson, and D. F. Shriver, *MRS Bull.*, 2000, 31–37.

27. M. Doyle, T. F. Fuller, and J. Newman, *Electrochim. Acta*, 1994, **39**, 2073–2081.
28. Y. Tominaga and K. Yamazaki, *Chem. Commun.*, 2014, **50**, 4448–4450.
29. B. Sun, J. Mindemark, K. Edström, and D. Brandell, *Electrochem. Commun.*, 2015, **52**, 71–74.
30. B. Sun, J. Mindemark, K. Edström, and D. Brandell, *Solid State Ionics*, 2013, 2–6.
31. J. Mindemark, E. Törmä, B. Sun, and D. Brandell, *Polymer*, 2015, **63**, 91–98.
32. M. Matsumoto, T. Uno, M. Kubo, and T. Itoh, *Ionics*, 2012, **19**, 615–622.
33. M. Forsyth, A. L. Tipton, D. F. Shriver, M. A. Ratner, and D. R. MacFarlane, *Solid State Ionics*, 1997, **99**, 257–261.
34. M. M. Silva, S. C. Barros, M. J. Smith, and J. R. MacCallum, *Electrochim. Acta*, 2004, **49**, 1887–1891.
35. S. E. Sloop, J. B. Kerr, and K. Kinoshita, *J. Power Sources*, 2003, **119-121**, 330–337.
36. P. B. Balbuena and Y. Wang, Eds., *Lithium-ion Batteries: Solid-Electrolyte Interphase*, Imperial College Press, London, 2004.
37. K. Edström, T. Gustafsson, and J. O. Thomas, *Electrochim. Acta*, 2004, **50**, 397–403.
38. Y. Yamada, Y. Iriyama, T. Abe, and Z. Ogumi, *Langmuir*, 2009, **25**, 12766–12770.
39. P. Verma, P. Maire, and P. Novák, *Electrochim. Acta*, 2010, **55**, 6332–6341.
40. K. Xu and von A. Cresce, *J. Mater. Chem.*, 2011, **21**, 9849.
41. A. M. Andersson, M. Herstedt, A. G. Bishop, and K. Edström, *Electrochim. Acta*, 2002, **47**, 1885–1898.
42. D. Aurbach, B. Markovsky, I. Weissman, E. Levi, and Y. Ein-Eli, *Electrochim. Acta*, 1999, **45**, 67–86.
43. S. Malmgren, K. Ciosek, R. Lindblad, S. Plogmaker, J. Kühn, H. Rensmo, K. Edström, and M. Hahlin, *Electrochim. Acta*, 2013, **105**, 83–91.
44. C. Xu, F. Lindgren, B. Philippe, M. Gorgoi, F. Björefors, K. Edstrom, and T. Gustafsson, *Chem. Mater.*, 2015, 10.1021/acs.chemmater.5b00339.
45. G. Gachot, S. Grugeon, M. Armand, S. Pilard, P. Guenot, J. M. Tarascon, and S. Laruelle, *J. Power Sources*, 2008, **178**, 409–421.
46. C. M. Ghimbeu, C. Decaux, P. Brender, M. Dahbi, D. Lemordant, E. Raymundo-Piñero, M. Anouti, F. Béguin, and C. Vix-Guterl, *J. Electrochem. Soc.*, 2013, **160**, A1907–A1915.
47. K. Leung and J. L. Budzien, *Phys. Chem. Chem. Phys.*, 2010, **12**, 6583–6586.
48. O. Borodin, G. R. V Zhuang, P. N. Ross, and K. Xu, *J. Phys. Chem. C*, 2013, **117**, 7433–7444.
49. R. Bouchet, S. Lascaud, and M. Rosso, *J. Electrochem. Soc.*, 2003, **150**, A1385–A1389.
50. G. B. Appetecchi, S. Scaccia, and S. Passerini, *J. Electrochem. Soc.*, 2000, **147**, 4448–4452.
51. Q. Li, H. Y. Sun, Y. Takeda, N. Imanishi, J. Yang, and O. Yamamoto, *J. Power Sources*, 2001, **94**, 201–205.
52. C. Xu, B. Sun, T. Gustafsson, K. Edström, D. Brandell, and M. Hahlin, *J. Mater. Chem. A*, 2014, **2**, 7256–7264.
53. M. Gemmei-Ide, T. Motonaga, and H. Kitano, *Langmuir*, 2006, **22**, 2422–2425.
54. L. Gireaud, S. Grugeon, S. Pilard, P. Guenot, J. M. Tarascon, and S. Laruelle, *Anal. Chem.*, 2006, **78**, 3688-3698.
55. X. Zhang, R. Kostecki, T. J. Richardson, J. K. Pugh, and P. N. Ross, *J. Electrochem. Soc.*, 2001, **148**, A1341-A1345.
56. G. Rokicki, *Prog. Polym. Sci.*, 2000, **25**, 259-342.
57. D. Aurbach and A. Schechter, *Electrochim. Acta*, 2001, **46**, 2395-2400.
58. A. M. Andersson, A. Henningson, H. Siegbahn, U. Jansson, and K. Edström, *J. Power Sources*, 2003, **119-121**, 522-527.
59. D. A. Wynn, M. M. Roth, and B. D. Pollard, *Talanta,* 1984, **31**, 1036–1040.
60. M. Nakayama, S. Wada, S. Kuroki, and M. Nogami, *Energy Environ. Sci.*, 2010, **3**, 1995-2002.

Graphic:

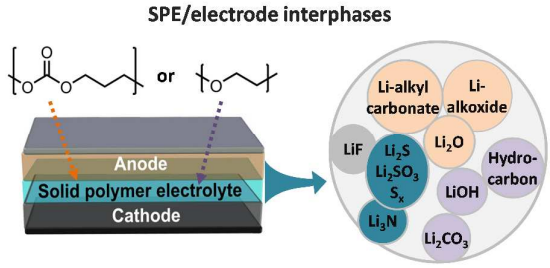

Highlight:

Compositional studies on interphase layers at polymer electrolyte/electrode interfaces displayed dependence on the host materials and its water content.